Journal of chemical & engineering data

Article

pubs.acs.org/jced

Adsorption of Cu(II), Pb(II), and Cd(II) Ions from Acidic Aqueous Solutions by Diethylenetriaminepentaacetic Acid-Modified Magnetic Graphene Oxide

Xin Li,*[,†,‡] Shengfan Wang,[†,‡] Yunguo Liu,[†,‡] Luhua Jiang,[†,‡] Biao Song,[†,‡] Meifang Li,[†,‡] Guangming Zeng,[†,‡] Xiaofei Tan,[†,‡] Xiaoxi Cai,[†,‡] and Yang Ding[†,‡]

[†]College of Environmental Science and Engineering, Hunan University, Changsha 410082, P.R. China

[‡]Key Laboratory of Environmental Biology and Pollution Control (Hunan University), Ministry of Education, Changsha 410082, P.R. China

Supporting Information

ABSTRACT: In this study, diethylenetriaminepentaacetic acid (DTPA)-modified magnetic graphene oxide (MGO) was synthesized for removal of Cu(II), Pb(II), and Cd(II) ions from acidic aqueous solutions. The prepared DTPA/MGO composites were characterized by scanning electron microscopy, X-ray diffraction, Fourier transform infrared and X-ray photoelectron spectroscopies, and zeta potential. The results showed that DTPA successfully functionalized MGO. Adsorption experiments indicated that DTPA/MGO composites exhibited excellent adsorption property in acidic aqueous solutions. The adsorption processes were applicable for the Langmuir adsorption isotherm and the pseudo-second-order model. The maximum adsorption capacities at pH 3.0 for Cu(II), Pb(II), and Cd(II) ions were 131.4, 387.6, and 286.5 mg/g, respectively. The thermodynamic studies demonstrated that adsorption processes were endothermic and spontaneous. Moreover, the DTPA/MGO composites could selectively adsorb Pb(II) from multimetal mixed systems. Adsorption−desorption results showed that the DTPA/MGO composites exhibited excellent reusability. These results suggested that DTPA/MGO composites have great potential in removing heavy metals from acidic wastewater, especially for Pb(II).

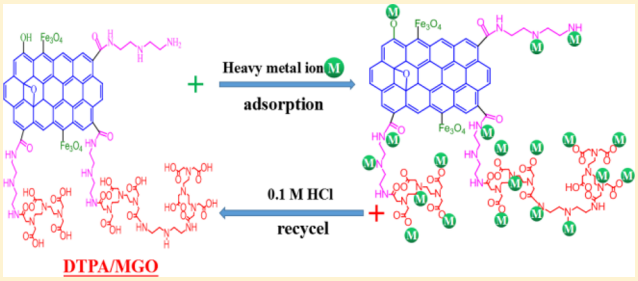

INTRODUCTION

Heavy metal contamination of water is an important environmental issue all over the world. It may cause serious health risks toward human beings such as kidney damage, emphysema, hypertension, neurological effects, and even cancer.[1−3] Therefore, it is necessary to take effective measures to deal with the heavy metal pollution in wastewater. Up to now, a number of methods have been used to remove heavy metals from contaminated water, including filtration,[4] precipitation,[5] biological treatment,[6] ion exchange,[7] etc. Besides, adsorption is regarded as the most promising approach considering that it is highly effective, relatively low-cost, flexible in design and simple in operation.[8] Numerous adsorbents have been developed to deal with the heavy metal pollution in wastewater such as activated carbon,[9] nanoadsorbents,[10] zeolite,[11] chitosan,[12] and biochar.[13]

In recent years, graphene oxide (GO) has attracted widespread attention because of its excellent physical-chemical properties. There are a number of researches focusing on using GO as an adsorbent to remove heavy metals from contaminated water.[14−16] GO can be obtained from the oxidation of graphene, and it contains various functional groups such as carboxyl, hydroxyl, and carbonyl,[17] which are effective functional groups to combine with heavy metals. However, there are some limitations in using GO as adsorbent to remove heavy metals directly. First, the separation of GO after adsorption is very difficult due to the preferable water solubility of GO. Second, GO shows good adsorption capacity for heavy metals from wastewater only under suitable pH condition (about pH = 6),[14] but the actual wastewater containing heavy metals is generally acidic.[8] To solve these problems, a large number of materials were used to modify the GO such as poly(acrylamide),[18] polyamidoamine,[19] chitosan,[20] β-cyclodextrin,[21] ethylenediaminetriacetic acid,[22] and ethylenediaminetetraacetic acid (EDTA).[23]

Diethylenetriaminepentaacetic acid (DTPA) is a kind of common chelating agent for heavy metal removal and contains five carboxylate groups bound to three nitrogen atoms. Hence, it has a strong ability to react with heavy metals. Furthermore, most species of DTPA are H_2DTPA^{3-}, H_3DTPA^{2-}, and H_4DTPA^{-} in acidic aqueous solutions, which still have the ability to combine with heavy metal ions.[24] The formations of

Received: August 21, 2016
Accepted: November 2, 2016
Published: November 10, 2016

ACS Publications © 2016 American Chemical Society

DOI: 10.1021/acs.jced.6b00746
J. Chem. Eng. Data 2017, 62, 407−416

Scheme 1. Synthesis Processes and Chemical Structure of DTPA/MGO Composites[a]

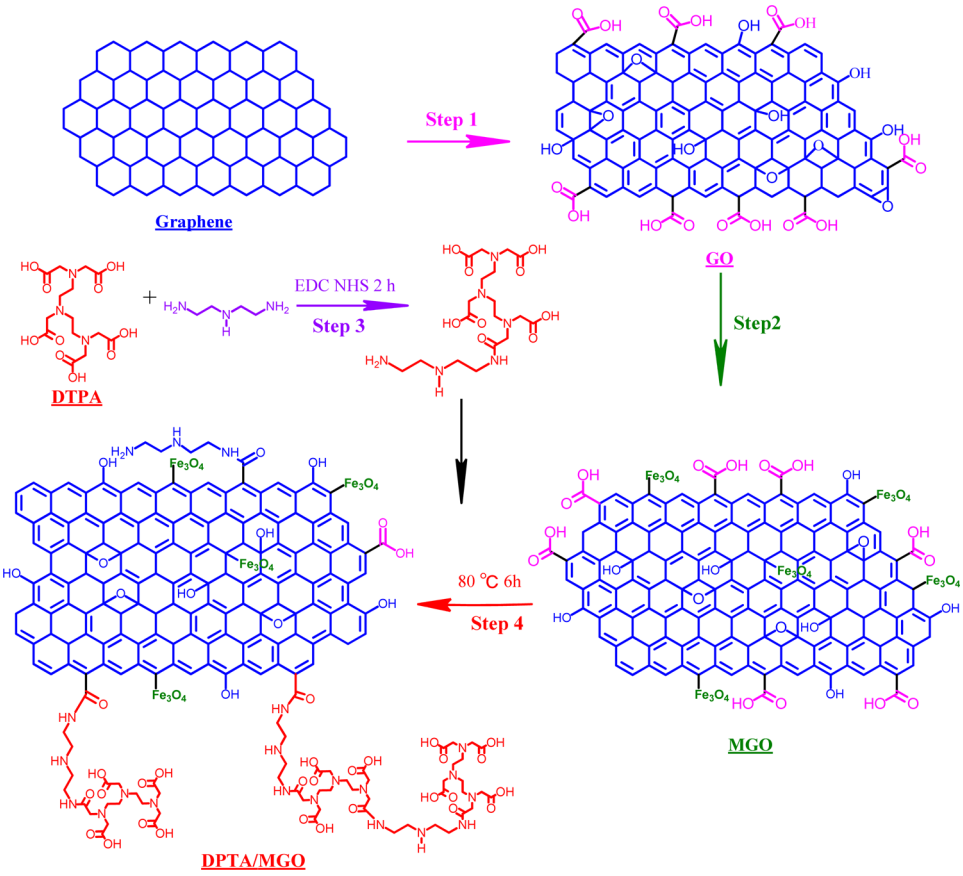

[a](Step 1) synthesis of GO (Step 2) by chemical co-precipitation method to obtain MGO; (Step 3) process of the activation of intermediates of DTPA; (Step 4) synthesis of DTPA/MGO composites.

these complexes are similar to that of EDTA, but they possess higher stability when complexed with heavy metals,[25] and the process exhibits high adsorption efficiency in acidic wastewater. Besides, the amine group has a highly reactive activity and can easily react with many other functional groups.[26] Therefore, DTPA can be used to modify GO via diethylenetriamine as a cross-linker.

In this work, to facilitate GO to separate from an aqueous solution after adsorption, magnetic nanoparticles were loaded on GO to synthesize magnetic graphene oxide (MGO).[27] Meanwhile, DTPA was grafted onto MGO via diethylenetriamine through an amidation reaction. To our knowledge, no research that used DTPA to modify magnetic graphene oxide was observed in previous literature. Thus, this study aims to demonstrate the possibility of DTPA/MGO composites as a promising adsorbent for the removal of heavy metal ions from acidic aqueous solutions and to provide insight into Cu(II), Pb(II), and Cd(II) ions adsorption from acidic aqueous solutions on the basis of isotherm, kinetics, and thermodynamic analysis.

EXPERIMENTAL SECTION

Materials. Graphite powder and diethylenetriamine were obtained from Sinopharm Chemical Reagent Co., Ltd. (Shanghai, China). 1-Ethyl-3-(3-dimethylaminoprophy) carbondiimide hydrochloride (EDC) and *N*-hydroxyl succinimide (NHS) were purchased from Civi Chemical Technology Co., Ltd. (Shanghai, China). DTPA was supplied by Xiya Reagent Research Center (Shandong, China). All other chemicals are analytical grade and used as received. The desired concentration of Cu(II), Pb(II), and Cd(II) ions solutions were obtained by diluting of 1000 mg/L Cu(II), Pb(II), and Cd(II) stock solution (see Supporting Information, Table S1).

Preparation of GO. GO was synthesized from natural graphite by a modified Hummer's method.[28] Briefly, natural graphite powders (6 g) was first preoxidized by mixed $K_2S_2O_8$ (5 g) and P_2O_5 (5 g) with H_2SO_4 (24 mL), and stirred at 80 °C for 6 h. After, the products were washed with ultrapure water until the solution became neutral and dried in a 60 °C vacuum oven for 12 h. The obtained preoxidized graphite and 5 g of $NaNO_3$ were slowly added to 240 mL of concentrated H_2SO_4 in a round-bottomed flask under stirring. Meanwhile, $KMnO_4$ (30 g) was gradually added at three different times. The dispersion was kept in an ice bath to maintain the temperature below 10 °C and stirred for 4 h. Then the temperature was raised to 35 °C for 2 h, and 500 mL of ultrapure water was slowly added with continuous stirring. Next, the temperature was increased to 98 °C for 1 h. After, this mixture was diluted by adding 1000 mL of ultrapure water at room temperature. Subsequently, 40 mL of 30% H_2O_2 was dropwise added to remove the redundant MnO_4^-, and the mixture was washed with 10% HCl until impurity ions were completely removed. Finally, the product was washed to neutral with excessive ultrapure water, and was sonicated for 2 h to obtain GO dispersion.

DOI: 10.1021/acs.jced.6b00746
J. Chem. Eng. Data 2017, 62, 407−416

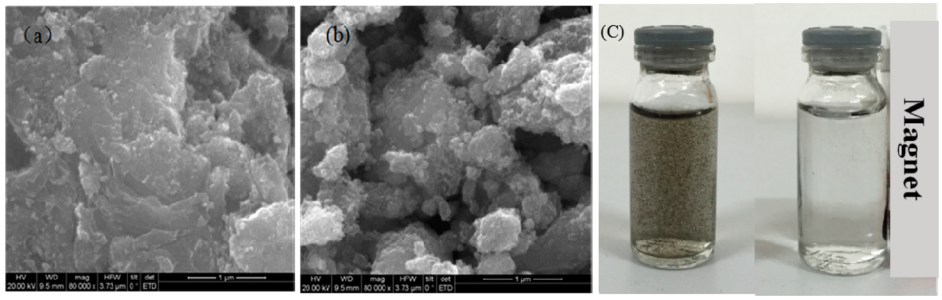

Figure 1. SEM images of MGO (a) and DTPA/MGO (b); magnetic susceptibility of the DTPA/MGO (c).

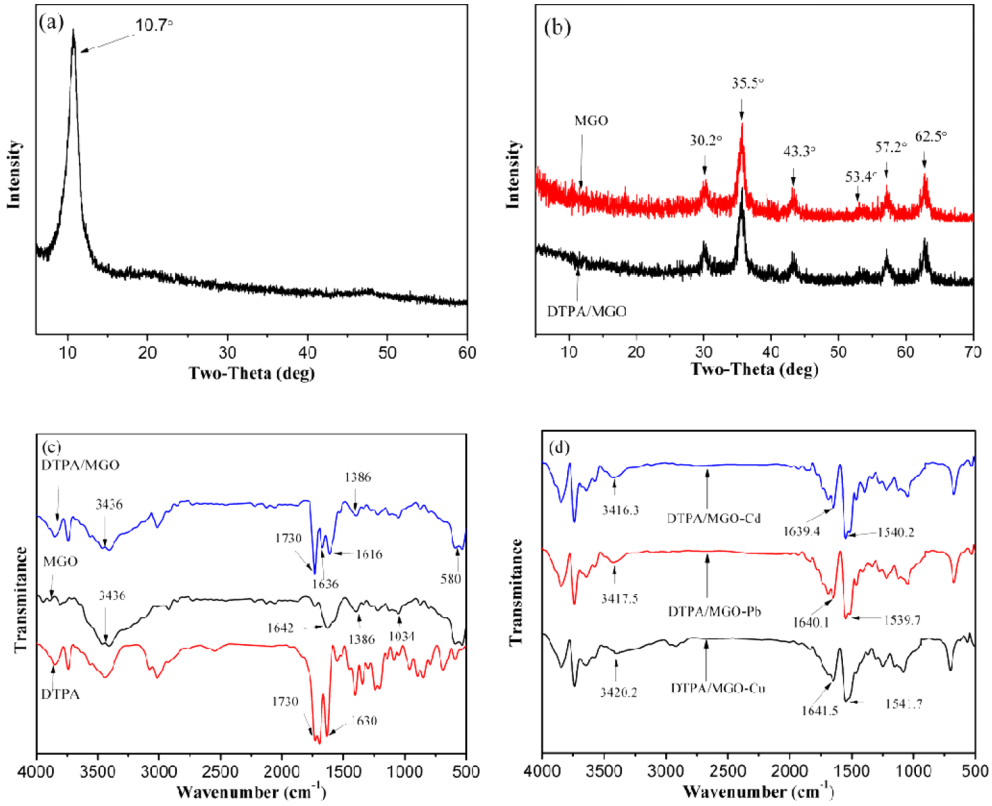

Figure 2. XRD patterns of GO (a), MGO and DTPA/MGO (b); FT-IR spectra of the GO, MGO, DTPA/MGO (c) and DTPA/MGO after adsorbed Cu(II), Pb(II), and Cd(II) ions (d).

Preparation of DTPA/MGO Composites. MGO was obtained by the coprecipitation method.[27] First, 200 mL of 0.05 M Fe^{2+} and 0.1 M Fe^{3+} mixture was added to 1000 mL of 2 mg/mL GO solution under continuous stirring. Then, 150 mL of ammonia was dispersed into the mixed solution and the mixture was continuously stirred in an 85 °C water bath for 45 min to form Fe_3O_4−GO composites. The DTPA/MGO composites were synthesized by an amidation reaction between DTPA and MGO via diethylenetriamine as a cross-linker.[29] The DTPA (800 mg) was dissolved in 400 mL of low-concentration ammonia solution. Next, 20 mL of 0.1 M EDC and 20 mL of 0.1 M NHS were added to the solution under continuous stirring for 2 h,[30] then 10 mL of diethylenetriamine was dropwise added. After that, the mixture was added into 2.0 g of MGO dispersion with continuous stirring in an 80 °C water bath for 6 h. After being cooled to room temperature, the resulting product was separated by a permanent magnet and washed repeatedly with ultrapure water until the solution was about neutral. Finally, the product was dried in a freeze drier and stored in a desiccator for the following experiments. The synthesis processes of DTPA/MGO composites are described in Scheme 1.

Characterization. The surface morphology of the MGO and DTPA/MGO composites were analyzed by scanning electron microscopy (SEM, Tecnai G2 F20, USA). The magnetic properties of the DTPA/MGO composites were tested by using a permanent magnet directly. The spacing structures of GO, MGO, and DTPA/MGO were recorded by using an X-ray diffractometer (XRD, Rigaku D/max-2500, Japan). FT-IR spectra of the DTPA, MGO, DTPA/MGO, and DTPA/MGO composites after being adsorbed were measured on a spectrophotometer (Varian 3100, USA). The XPS measurements of the MGO and DTPA/MGO composites were performed by using an X-ray photoelectron spectrometer (Escalab 250 xi Thermo Fisher, USA). The zeta potential of DTPA/MGO composites was measured on a zetasizer (ZEN3600 UK) at different pH values.

DOI: 10.1021/acs.jced.6b00746
J. Chem. Eng. Data 2017, 62, 407−416

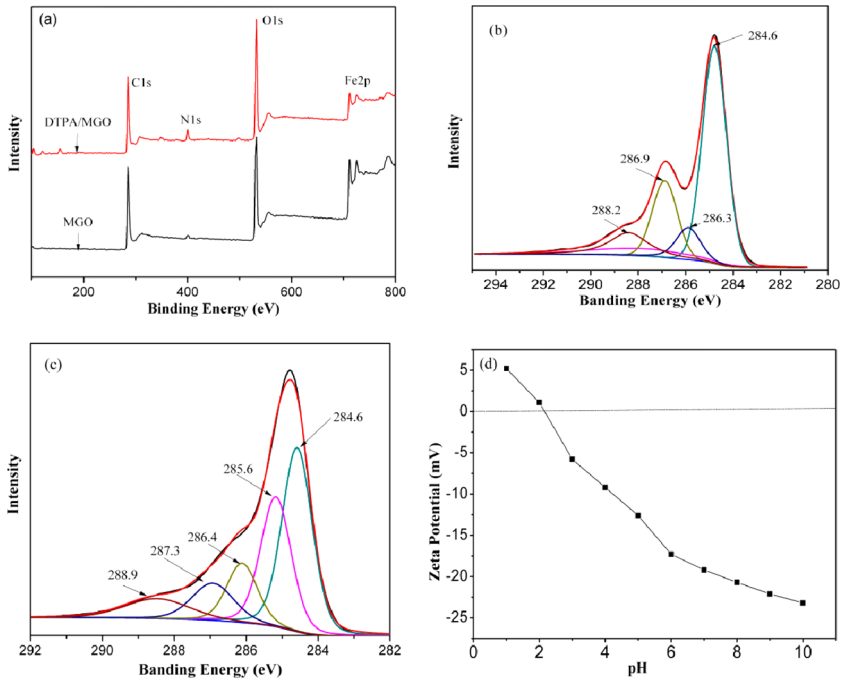

Figure 3. XPS spectra of MGO and DTPA/MGO (a); C 1s XPS spectra of MGO (b); and DTPA/MGO (c); zeta potential of DTPA/MGO (d).

Batch Adsorption Experiments. Adsorption experiments were performed by adding 10 mg of DTPA/MGO composites to 50 mL conical flasks containing 25 mL of Cu(II), Pb(II), and Cd(II) ions solution. Then, the flasks were placed in a 20 °C water bath shaker that was operated at 180 rpm for 24 h. The experimental procedures to determined the influence of the pH value of the solution on adsorption processes were as follows: 10 mg of DTPA/MGO composites was added into 25 mL of 100 mg/L Cu(II), Pb(II), and Cd(II) ions solution, respectively. Different concentrations of HCl or NaOH solutions (0.01−1.0 M) were used to adjust the initial pH values of solutions from 1.5 to 6.0. As a comparison, similar experiments were also conducted by adding 10 mg of MGO. The adsorption isotherm experiments were analyzed by adding 10 mg of DTPA/MGO composites to solutions; the initial Cu(II) and Cd(II) ions concentrations varied from 10 mg/L to 300 mg/L and the concentration of Pb(II) varied from 10 mg/L to 400 mg/L. For the adsorption kinetic analysis, 40 mg of DTPA/MGO composites were added into 100 mL of 100 mg/L Cu(II), Pb(II), and Cd(II) ions solution with a contact time ranging from 0 to 360 min. The samples were taken for Cu(II), Pb(II), and Cd(II) ions concentration measurements at specific time intervals. Then, the mixtures after adsorption were separated by a permanent magnet and filtered through a 0.22 μm aperture of the membrane; the concentrations of metal ions in the filtrate were measured by atomic adsorption spectroscopy (PerkinElmer AA700, USA). The adsorption capacity (q_e, mg/g) was calculated by the following equation:

$$Q_e = [(C_0 - C_e)V]/m \quad (1)$$

where C_0 and C_e are initial and final concentrations of the solution (mg/L); V is the initial volume of the solution (L); m is the mass of adsorbent (g).

RESULTS AND DISCUSSION

Characterization of DTPA/MGO. The surface characteristics of MGO and DTPA/MGO composites are shown in Figure 1. The images clearly show that the DTPA/MGO composites had a relatively rougher surface than MGO, which might be due to the immobilization of DTPA onto the surface of the MGO layers. It can be concluded that the rough DTPA/MGO composites process a larger special surface, which might be beneficial for bonding more heavy metal ions. The magnetic susceptibility of the DTPA/MGO composites is demonstrated in Figure 1c. It showed that the DTPA/MGO composites (0.4 mg/mL) could be recovered completely from the aqueous solution through a permanent magnet. This indicated that DTPA/MGO had good magnetism, could be recycled by a magnet, and would not cause repollution.

Figure 2 illustrates the XRD patterns of GO, MGO, and DTPA/MGO composites. For GO, a strong peak at $2\theta = 10.7°$ occurred, which was due to many oxygen-containing functional groups on the surface of GO. These results were consistent with the previous study.[31] For MGO and DPTA/MGO composites, the peaks at 30.2°, 35.5°, 37.5°, 43.3°, 53.4°, 57.2°, and 62.5° were observable. These peaks correspond to the cubic spinel crystal planes of Fe_3O_4.[32] Compared with the XRD pattern of GO, the peak at $2\theta = 10.7°$ of GO vanished in the patterns of MGO and DPTA/MGO composites because the signals of the carbon peak are too weak and are covered up by iron oxides peaks. The XRD patterns of MGO and DPTA/MGO composites were almost similar, which indicated that no changes of the crystalline phase of Fe_3O_4 occurred in the synthesis process.

The FT-IR spectra of the DTPA, MGO, and DTPA/MGO composites are shown in Figure 2c. The FT-IR spectrum of DTPA showed that a strong peak appeared at 1730 cm^{-1}, which indicated the existence of abundant carboxyl groups in DTPA. In the spectrum of MGO, the peak at 3436 cm^{-1} indicated the presence of O−H. The peak at 1642 cm^{-1} was attributed to the stretching vibration of $-COO^-$, which may be derived from the −COOH on the Fe_3O_4-coated GO.[29] The peak appearing at 580 cm^{-1} is associated with the Fe−O stretching vibration, while in the FT-IR spectrum of DPTA/

DOI: 10.1021/acs.jced.6b00746
J. Chem. Eng. Data 2017, 62, 407−416

MGO composites, −COOH, −NHCO−, and N−H bonds appear at 1730, 1636, and 1616 cm^{-1}, respectively.[33] The peaks at 1384 and 1035 cm^{-1} corresponded to C−OH and C−O−C stretching vibration, respectively. After chemical grafting was performed, the spectra showed the new vibration peaks at 1730, 1636, and 1616 cm^{-1} due to DTPA and diethylenetriamine grafted onto the surface of MGO. The FT-IR spectra of the DTPA/MGO after adsorption are shown in Figure 2d. The results showed that the peaks of DTPA/MGO composites at 3440 cm^{-1} from O−H, 1730 cm^{-1} from carboxyl, and at 1636 cm^{-1} from carbonyl changed significantly after absorbing heavy metal ions. This suggested that those functional groups were involved in the reaction with heavy metals, which led to the changes of the original peaks.

The chemical speciation of elements in MGO and DPTA/MGO composites was further confirmed by XPS. The full scan XPS spectrum (Figure 3a) of DPTA/MGO composites showed that the peaks at 711, 533, 400, and 285 eV belonged to Fe 2p, O 1s, N 1s, and C 1s, respectively.[34] Comparing the XPS results of atomic content DPTA/MGO composites to MGO, we found that that element content of C, O, N, and Fe at DPTA/MGO composites were 53.28, 37.36, 5.13, and 4.23%, respectively. The element content of C, O, N, and Fe at MGO were 58.42, 32.25, 0.96, and 8.37%, respectively. It indicated that the amount of N 1s was significantly increased, which was originated from diethylenetriamine and DPTA. The O/C atomic ratio of DPTA/MGO composites (0.70) was considerable higher than MGO (0.55), which might be attributed to the high oxygen content of the introduced DPTA.

In the C 1s spectrum of MGO (Figure 3b), four obvious peaks appeared at 288.2, 286.9, 286.3, and 284.6 eV, corresponding to C═O, C−O−C, C−O, and C−C groups of MGO, respectively.[35] The C 1s spectrum of DPTA/MGO composites (Figure 3c) shows five componential peaks at 288.9, 287.5, 286.5, 285.6, and 284.6 eV, which belonged to the bonds of −O−C═, −NHCO−, C−O, C−N, and C−C, respectively. Additional −O−C═, −NHCO−, and C−N bonds were observed. −O−C═ and C−N were originated from DTPA. The existence of −NHCO− adequately proved that the −COOH groups of DTPA were combined with the $-NH_2$ groups of diethylenetriamine. Thus, it indicated that DTPA had been grafted successfully to the MGO surface via diethylenetriamine.

The pHzpc (pH at point of zero charge Figure 3d) of DPTA/MGO composites estimated by electroacoustic spectrometry was approximately 2.2, which shows that the prepared DPTA/MGO composites are negatively charged when the pH value of the solution is greater than 2.2; this resulted in electrostatic interactions between DTPA/MGO composites and heavy metal ions.

Effect of Initial pH Value. The pH value of the solution is a very important factor in the process of adsorption. It has an impact on the surface charge and states of the binding sites of adsorbent. The effects of solution pH on the adsorption capacity of MGO and DTPA/MGO were investigated at pH values from 1.5 to 6, and the results are presented in Figure 4. It is found that adsorption processes of MGO were strongly dependent on pH. The adsorption capacity of Cu(II), Pb(II), and Cd(II) ions were increased with the solution pH increasing from 1.5 to 6.0. As compared to MGO, the adsorption processes of DTPA/MGO composites were weakly affected by pH and excellent adsorption capacity was obtained at pH 3−6. This result was consistent with another study[36] and could be

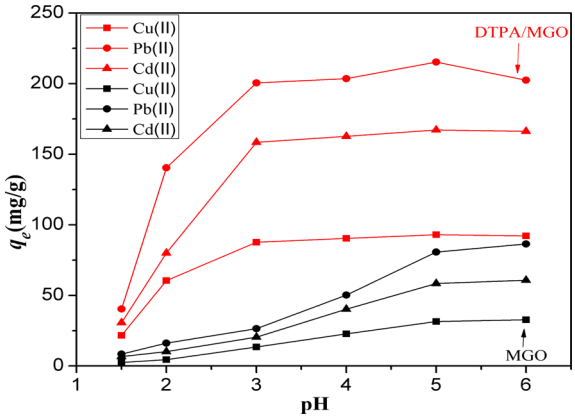

Figure 4. Effect of pH on adsorption behavior of Cu(II), Pb(II), Cd(II) onto MGO and DTPA/MGO. (C_0 = 100 mg/L, m/V = 0.4 mg/mL, T = 293 K, t = 24 h).

explained by the ionization degree and the surface charge of the adsorbent. Low pH inhibited the deprotonation of carboxyl and hydroxyl groups on MGO, which consequently weakened the electrostatic interaction between MGO and metal ions,[37] so it has low adsorption capacity under acidic conditions, but on the surface of DTPA/MGO composites, the carboxyl of MGO was modified by DTPA. When the pH is 2.5, the species of DTPA are H_2DTPA^{3-} (27.17%), H_3DTPA^{2-} (14.93%), H_4DTPA^{-} (54.39%), and H_6DTPA^{+} (3.51%).[24] Ignoring a very small part of the protonated species, the largest part of DTPA has the ability to form stable complexes with metal ions. This is the reason why the DTPA/MGO can achieve high adsorption properties in acid aqueous solution. Considering that the actual wastewater containing heavy metals is usually strongly acidic,[8] pH 3.0 was chosen as the experimental condition to investigate adsorption properties of DTPA/MGO composites under acidic condition.

Adsorption Isotherms. An adsorption isotherm expresses the relationship between adsorption capacity (q_e, mg/g) and concentration of adsorption equilibrium (C_e, mg/L). Figure 5

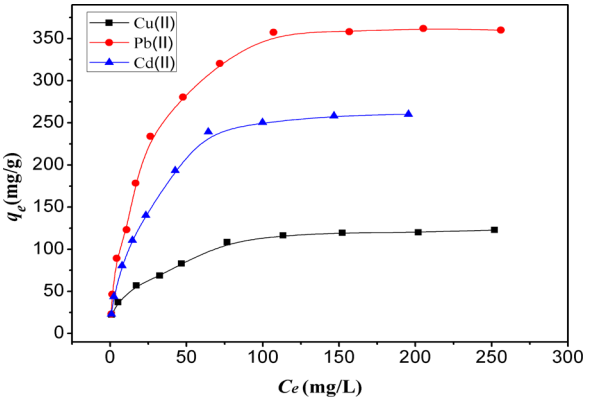

Figure 5. Adsorption isotherms of Cu(II), Pb(II), and Cd(II) ions on DTPA/MGO (pH = 3.0, m/V = 0.4 mg/mL, T = 293 K, t = 24 h).

shows Cu(II), Pb(II), and Cd(II) ions adsorption isotherms of DTPA/MGO composites. In this study, the experimental data of metals uptake onto DTPA/MGO composites were analyzed by Langmuir and Freundlich isotherms. The Langmuir model is expressed as follows:

DOI: 10.1021/acs.jced.6b00746
J. Chem. Eng. Data 2017, 62, 407−416

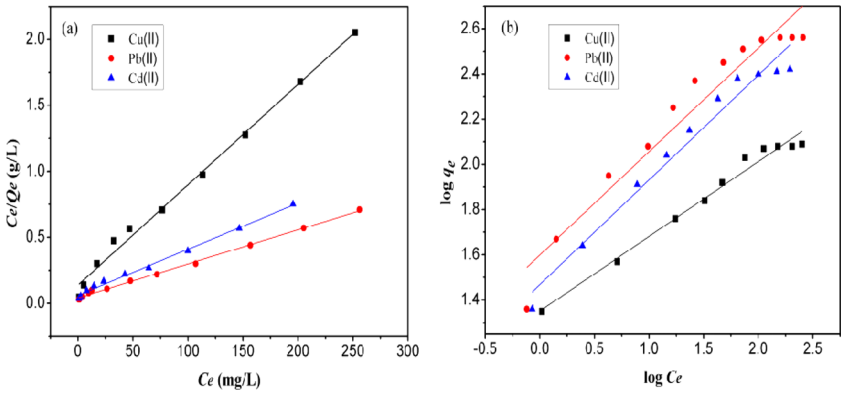

Figure 6. Langmuir (a) and Freundlich (b) isotherms for the adsorption of Cu(II), Pb(II), and Cd(II) ions on DTPA/MGO.

$$C_e/q_e = C_e/q_m + 1/(k_L q_m) \quad (2)$$

The Freundlich isotherm is described as follows:

$$\log q_e = \log k_F + (1/n) \log C_e \quad (3)$$

where C_e (mg/L) is the concentration of equilibrium; q_e (mg/g) is the equilibrium adsorption capacity; q_m (mg/g) is the maximum adsorption capacity corresponding to the Langmuir model; k_L (L/mg) is the Langmuir adsorption constant. K_F and n are Freundlich constants related to the adsorption capacity and adsorption intensity, respectively. The values of q_m and k_L can be derived from the slope and intercept of C_e/q_e versus C_e. The values of n and K_F can be obtained from the slope and intercept of log q_e versus log C_e.

The Langmuir and Freundlich isotherms parameters was obtained by means of linear fitting, as shown in Figure 6, and the calculated parameters are presented in Table 1. The value

Table 1. Parameters for the Langmuir and Freundlich Models of Cu(II), Pb(II), and Cd(II) Ions on DTPA/MGO (pH = 3.0, m/V = 0.4 mg/mL, T = 293 K, t = 24 h)

	Langmuir model			Freundlich isotherm		
metal ion	Q_{max} (mg/g)	K_L (L/mg)	R^2	K_F	$1/n$	R^2
Cu(II)	131.41	0.056	0.993	22.44	0.331	0.981
Pb(II)	387.59	0.063	0.997	39.72	0.458	0.934
Cd(II)	286.53	0.058	0.994	29.41	0.463	0.967

of the correlation coefficient is a criterion of fitting degree for the system. Table 1, it indicates that the Langmuir model (R^2 > 0.99) shows a better correlation than the Freundlich model (0.934 < R^2 < 0.981), indicating that the Langmuir model is more consistent in evaluating sorption equilibrium, which indicated that Cu(II), Pb(II), and Cd(II) ions adsorbed as a monolayer covering the DTPA/MGO composites. Furthermore, the values of K_L are between 0.056 and 0.063 (0 < K_L < 1), which impies that the adsorption processes are favorable. The q_m values calculated from the Langmuir model were 131.41, 387.60, and 286.53 mg/g for Cu(II), Pb(II), and Cd(II) ions, respectively. Comparing Q_{max} values of Cu(II), Pb(II), and Cd(II) ions adsorption to other adsorbents (Table 2), the results showed that the DTPA/MGO composites present a higher adsorption capacity.

Adsorption Kinetics. Figure 7 shows the adsorption kinetic of Cu(II), Pb(II), and Cd(II) ions by DTPA/MGO composites at different time intervals. In this study, the pseudo-first-order and the pseudo-second-order model were employed to analyze

Table 2. Comparison of the Maximum Adsorption Capacity of Cu(II), Pb(II), and Cd(II) Ions on Various Adsorbents

adsorbent	metal ions	Q_{max} (mg/g)	refs
amino-functionalized magnetic nanoparticles	Cu(II)	25.77	38
graphene oxide aerogel	Cu(II)	29.59	39
graphene oxide membranes	Cu(II)	72.6	14
graphene oxide/polyamidoamine	Cu(II)	68.68	40
modified bagasse	Cu(II)	101.01	41
graphene oxide	Cu(II)	117.5	16
DTPA/MGO	Cu(II)	131.41	this study
amino functionalized magnetic graphenes	Pb(II)	27.95	42
PAS-GO	Pb(II)	312.5	26
SMG	Pb(II)	6.00	43
LS-GO-PANI	Pb(II)	216.4	17
magnetic chitosan/graphene oxide	Pb(II)	76.41	44
L-tryptophan Functionalized GO	Pb(II)	222	45
DTPA/MGO	Pb(II)	387.6	this study
Grapheme oxide nanosheets	Cd(II)	44.64	8
graphene oxide membranes	Cd(II)	83.8	14
amino functionalized magnetic graphenes	Cd(II)	27.83	38
P(AANa-*co*-AM)/GO hydrogel	Cd(II)	196.4	46
kapok-DTPA	Cd(II)	163.7	36
magnetic graphene oxide	Cd(II)	91.29	37
DTPA/MGO	Cd(II)	286.56	this study

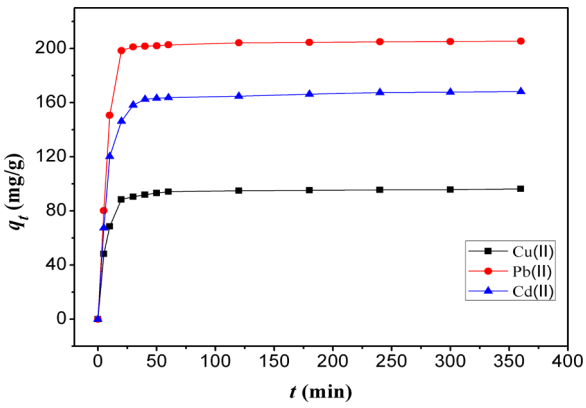

Figure 7. Effect of time on adsorption behavior of Cu(II), Pb(II), and Cd(II) ions on DTPA/MGO (C_0 = 100 mg/L, pH = 3.0, m/V = 0.4 mg/mL, T = 293 K).

DOI: 10.1021/acs.jced.6b00746
J. Chem. Eng. Data 2017, 62, 407−416

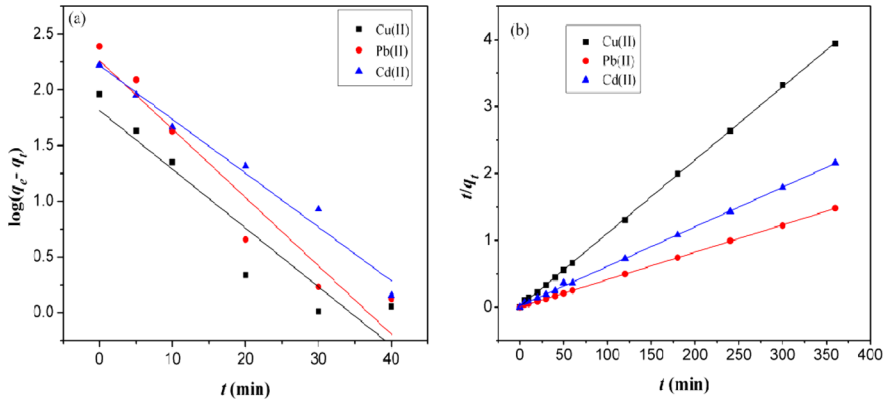

Figure 8. Pseudo-first-order (a) and pseudo-second-order models (b) for Cu(II), Pb(II), and Cd(II) ions on DTPA/MGO.

Table 3. Parameters for the Pseudo-First-Order and Pseudo-Second-Order Models of Cu(II), Pb(II), and Cd(II) Ions on DTPA/MGO

	pseudo-first-order			pseudo-second-order			
metal ion	q_e (cal) (mg/g)	K_1 (1/min)	R^2	q_e (cal) (mg/g)	K_2 (mg/g min)	R^2	$q_e$exp (mg/g)
Cu(II)	85.75	0.121	0.870	96.7	0.0143	0.9988	96.25
Pb(II)	186.5	0.141	0.919	207.03	0.0229	0.9992	205.5
Cd(II)	145.28	0.112	0.977	169.20	0.0204	0.9994	168.25

the kinetic models. The pseudo-first-order model kinetic equation is expressed as follows:

$$\log(q_e - q_t) = \log q_e - k_1 t/2.303 \quad (4)$$

The pseudo-second-order model kinetic equation is described as follows:

$$t/q_t = 1/k_2 q_e^2 + t/q_e \quad (5)$$

Where q_e (mg/g) is the equilibrium adsorption capacity; q_t (mg/g) is the adsorption capacity at time t; k_1 is the rates constant of the pseudo-first-order; k_2 is the rates constant of the pseudo-second-order model.

The adsorption kinetic plots showed that the adsorption reached adsorption equilibrium in a very short time, and most of the Cu(II), Pb(II), and Cd(II) ions were removed within 20 min. The cause of this phenomenon could be the strong attractive forces between Cu(II), Pb(II), and Cd(II) ions and DTPA, which leads to fast diffusion of Cu(II), Pb(II), and Cd(II) ions into the interlayer space of the DTPA/MGO. The linear fitting degrees of the two models are shown in Figure 8. The correlation coefficients calculated from the pseudo-first-order and the pseudo-second-order models are presented in Table 3. Comparing q_e with $q_{e,exp}$ for Cu(II), Pb(II), and Cd(II) ions. The q_e values obtained by the pseudo-second-order equation are 96.25 mg/g, 205.5 mg/g, and 168.25 mg/g, which are close to the values obtained by the experiment. However, the calculated q_e values obtained by the pseudo-first-order equation are not in agreement with the experimental q_e values, suggesting that the adsorption of Cu(II), Pb(II), and Cd(II) ions does not follow the pseudo-first-order kinetics. The values of the correlation coefficients of the pseudo-second-order model for Cu(II), Pb(II), and Cd(II) ions are 0.9988, 0.9992, and 0.9994, respectively. All of them are higher than the values obtained by the pseudo-first-order model. It vividly indicated that the applicable adsorption kinetics followed the pseudo-second-order model. These results indicated that the overall rates of the adsorption of Cu(II), Pb(II), and Cd(II) ions onto DTPA/MGO were controlled by chemical adsorption.

Thermodynamic Studies. Whether the adsorption process can be carried out spontaneously is determined by the energy and entropy of the reaction. The absorption isotherms were conducted under different temperature (293 to 323 K) to study the effects of temperature on adsorption capacity. The effects of temperature on Cu(II), Pb(II), and Cd(II) ions adsorption are presented in Figure 9. It can be seen that with the increase of temperature, the adsorption capacity is increasing, which meant that the adsorption process was endothermic. The thermodynamic parameters (ΔH^0, ΔS^0, and ΔG^0) for Cu(II), Pb(II), and Cd(II) ions adsorption on DTPA/MGO composites can be calculated using the following equations:[47]

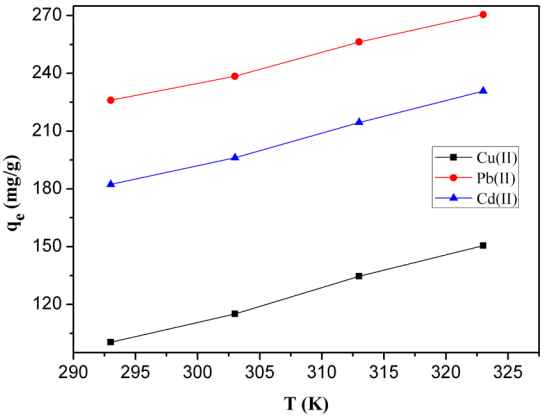

Figure 9. Effect of temperature on adsorption capacity (C_0 = 100 mg/L, pH = 3.0, m/V = 0.4 mg/mL, t = 24 h).

$$\ln K^0 = \Delta S^\circ/R - \Delta H^\circ/RT \quad (6)$$

$$\Delta G^\circ = -RT \ln K^0 \quad (7)$$

DOI: 10.1021/acs.jced.6b00746
J. Chem. Eng. Data 2017, 62, 407−416

$$K^0 = q_e/C_e \quad (8)$$

T is the temperature of the solution (in Kelvin), R is the gas constant (8.314 J·mol^{-1} K^{-1}), and K^0 is the thermodynamic equilibrium constant. Thermodynamic parameters were calculated according to eqs 6−8. Linear fitting of ln K^0 vs $1/T$ for the adsorption of Cu(II), Pb(II), and Cd(II) ions on DTPA/MGO composites were described in Figure 10. The values of $\Delta H^0/R$

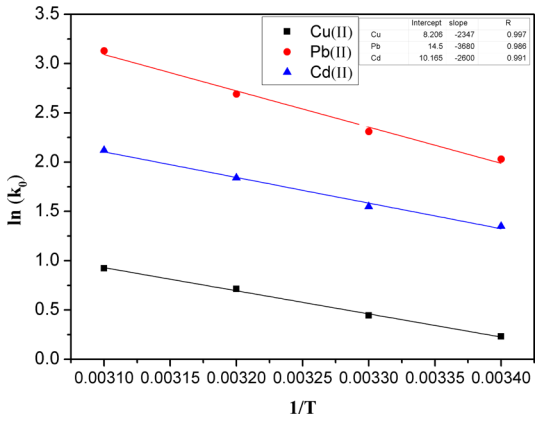

Figure 10. Linear plot of ln K^0 vs $1/T$ for the adsorption of Cu(II), Pb(II), and Cd(II) ions on DTPA/MGO.

and $\Delta S^0/R$ are equal and the slope and intercept by ln K^0 against $1/T$ gives a straight line, respectively. The results are shown in Table 4. The negative values of ΔG^0 indicated that

Table 4. Thermodynamic Parameters of Cu(II), Pb(II), and Cd(II) Ions Adsorption on DTPA/MGO

metal ion	T (K)	ΔG (kJ/mol)	ΔS (kJ (K^{-1}/mol))	ΔH (J/mol)	R^2
Cu(II)	293	−2.436	19.52	68.23	0.996
	303	−2.567			
	313	−2.682			
	323	−2.863			
Pb(II)	293	−7.552	30.60	120.57	0.986
	303	−7.802			
	313	−8.306			
	323	−8.685			
Cd(II)	293	−5.116	21.62	84.52	0.991
	303	−5.238			
	313	−5.405			
	323	−5.571			

the adsorption processes are spontaneous. The positive values of ΔH^0 confirmed the endothermic nature of the overall adsorption processes and positive values of ΔS^0 suggested that the random nature of the solid/solution interface increased during the adsorption processes.

Selective Adsorption Test. In most cases, there are several heavy metal ions coexisting in wastewater. Therefore, it is necessary to test the adsorption performance of an adsorbent in a multimetal system. In this study, the competitive adsorption of Pb(II), Cu(II), Cd(II), Zn(II), and Ni(II) ions mixed solution onto DTPA/MGO composites was conducted. A 40 mg sample of DTPA/MGO composites was added to 100 mL of solution that contained 100 mg/L of each kind of metal. For comparison, a similar experiment was carried out in 100 mg/L Pb(II) solutions. The results are shown in Figure 11 where it

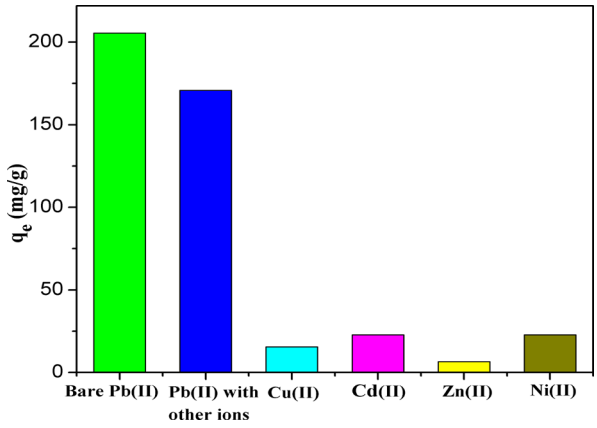

Figure 11. Selective adsorption properties of DTPA/MGO.

can be seen that the DTPA/MGO composites showed excellent adsorption selectivity for Pb(II) ions. This may be because the high ionic radius of Pb(II) ions led to the formation of a more distorted structure between DTPA chelates and Pb(II) ions, which was more likely to occur in the complex reaction.[48] In addition, under the condition of the existence of other heavy metal ions, the adsorption capacity of DTPA/MGO composites to Pb(II) decreased slightly, which is due to the competition for adsorption sites between coexisting ions and Pb(II). The results suggested that Pb(II) ions could be separated from wastewater containing Cu(II), Zn(II), Ni(II), and Cd(II) ions by using DTPA/MGO composites.

Desorption and Reuse Studies. Taking the practical application into account, an ideal adsorbent should show good regeneration ability and high adsorption capacity. In this study, the DTPA/MGO composites of adsorbed Cu(II), Pb(II), and Cd(II) ions were collected by a permanent magnet and thoroughly rinsed with ultrapure water. Then, they were placed in 0.1 M HCl solution under stirring for desorption. The regenerated DTPA/MGO composites were dried in a freeze drier and used for adsorption−desorption experiments. As shown in Figure 12, the total adsorption capacity of DTPA/MGO composites for Cu(II), Pb(II), and Cd(II) ions after six cycles decreased approximately 8.2%, 15.5%, and 10.3%, respectively. The slight decrease in the adsorption capacity may be due to the loss of the binding sites on the surface of the adsorbent during the process of adsorption and desorption. The adsorption−desorption results indicated that the prepared

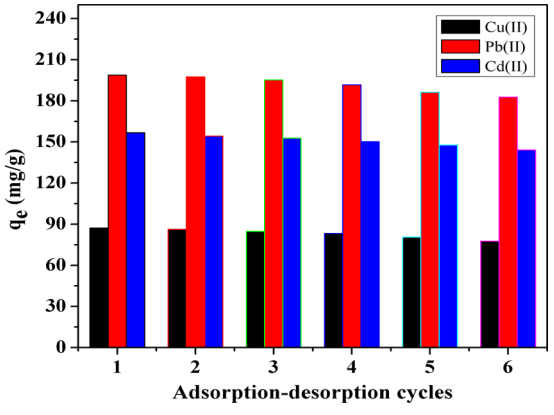

Figure 12. Adsorption−desorption cycles of Cu(II), Pb(II), and Cd(II) ions adsorption on DTPA/MGO.

DOI: 10.1021/acs.jced.6b00746
J. Chem. Eng. Data 2017, 62, 407−416

DTPA/MGO composites could be an ideal heavy metal adsorbents.

CONCLUSIONS

A new adsorbent, DTPA/MGO composites, has been successfully prepared by an amidation reaction between DTPA and MGO through diethylenetriamine as a cross-linker. The prepared DTPA/MGO composites had much higher adsorption capacity than original MGO. The maximum adsorption capacities obtained from the Langmuir model for Cu(II), Pb(II), and Cd(II) ions were 131.4, 387.6, and 286.5 mg/g, respectively. Cu(II), Pb(II), and Cd(II) ions adsorption on DTPA/MGO was weakly dependent on pH, and the adsorbents also have great adsorption capacity under acidic conditions. The adsorption process is fast which could reach adsorption equilibrium within 20 min and follow the pseudo-second-order kinetic model. The thermodynamic studies demonstrated that adsorption processes were endothermic and spontaneous. What is more, the DTPA/MGO composites showed great adsorption selectivity for Pb(II) and exhibited excellent reusability. On the basis of the experimental results, DTPA/MGO composites can be a potentially suitable material for removal of heavy metals from acidic aqueous solutions, especially for Pb(II).

ASSOCIATED CONTENT

Supporting Information

The Supporting Information is available free of charge on the ACS Publications website at DOI: 10.1021/acs.jced.6b00746.

Tables of basic information on reagents and possible adsorption mechanism of Cu(II), Pb(II), and Cd(II) ions on DTPA/MGO composites (PDF)

AUTHOR INFORMATION

Corresponding Author

*Tel.: +86 731 88649208. Fax: +86 731 88822829. E-mail: hgxlixin@hnu.edu.cn.

Funding

This research was supported by the National Natural Science Foundation of China (Grant no.51521006 and 51579097).

Notes

The authors declare no competing financial interest.

REFERENCES

(1) Jacob, B.; Ritz, B.; Heinrich, J.; Hoelscher, B.; Wichmann, H. E. The effect of low-level blood lead on hematologic parameters in children. *Environ. Res.* **2000**, *82*, 150−159.

(2) Mates, J. M.; Segura, J. A.; Alonso, F. J.; Marquez, J. Roles of dioxins and heavy metals in cancer and neurological diseases using ROS-mediated mechanisms. *Free Radical Biol. Med.* **2010**, *49*, 1328−1341.

(3) Cao, C. Y.; Qu, J.; Wei, F.; Liu, H.; Song, W. G. Superb adsorption capacity and mechanism of flowerlike magnesium oxide nanostructures for lead and cadmium ions. *ACS Appl. Mater. Interfaces* **2012**, *4*, 4283−4287.

(4) Lakard, S.; Magnenet, C.; Mokhter, M. A.; Euvrard, M.; Buron, C. C.; Lakard, B. Retention of Cu(II) and Ni(II) ions by filtration through polymer-modified membranes. *Sep. Purif. Technol.* **2015**, *149*, 1−8.

(5) Chen, Q.; Luo, Z.; Hills, C.; Xue, G.; Tyrer, M. Precipitation of heavy metals from wastewater using simulated flue gas: Sequent additions of fly ash, lime and carbon dioxide. *Water Res.* **2009**, *43*, 2605−2614.

(6) Wang, J.; Chen, C. Biosorbents for heavy metals removal and their future. *Biotechnol. Adv.* **2009**, *27*, 195−226.

(7) Mazur, L. P.; Pozdniakova, T. A.; Mayer, D. A.; Boaventura, R. A.; Vilar, V. J. Design of a fixed-bed ion-exchange process for the treatment of rinse waters generated in the galvanization process using Laminaria hyperborea as natural cation exchanger. *Water Res.* **2016**, *90*, 354−368.

(8) Xue, X.; Xu, J.; Baig, S. A.; Xu, X. Synthesis of graphene oxide nanosheets for the removal of Cd(II) ions from acidic aqueous solutions. *J. Taiwan Inst. Chem. Eng.* **2016**, *59*, 365−372.

(9) Parlayici, S.; Eskizeybek, V.; Avcı, A.; Pehlivan, E. Removal of chromium (VI) using activated carbon-supported-functionalized carbon nanotubes. *J. Nanostruct. Chem.* **2015**, *5*, 255−263.

(10) Petranovska, A. L.; Abramov, N. V.; Turanska, S. P.; Gorbyk, P. P.; Kaminskiy, A. N.; Kusyak, N. V. Adsorption of cis-dichlorodiammineplatinum by nanostructures based on single-domain magnetite. *J. Nanostruct. Chem.* **2015**, *5*, 275−285.

(11) Wang, S.; Peng, Y. Natural zeolites as effective adsorbents in water and wastewater treatment. *Chem. Eng. J.* **2010**, *156*, 11−24.

(12) Wan Ngah, W. S.; Teong, L. C.; Hanafiah, M. A. K. M. Adsorption of dyes and heavy metal ions by chitosan composites: A review. *Carbohydr. Polym.* **2011**, *83*, 1446−1456.

(13) Tan, X. F.; Liu, Y. G.; Zeng, G. M.; Wang, X.; Hu, X.; Gu, Y. L.; Yang, Z. Application of biochar for the removal of pollutants from aqueous solutions. *Chemosphere* **2015**, *125*, 70−85.

(14) Tan, P.; Sun, J.; Hu, Y.; Fang, Z.; Bi, Q.; Chen, Y.; Cheng, J. Adsorption of Cu(II), Cd(II) and Ni(II) from aqueous single metal solutions on graphene oxide membranes. *J. Hazard. Mater.* **2015**, *297*, 251−260.

(15) Zhang, F.; Song, Y.; Song, S.; Zhang, R.; Hou, W. Synthesis of magnetite-graphene oxide-layered double hydroxide composites and applications for the removal of Pb(II) and 2,4-dichlorophenoxyacetic acid from aqueous solutions. *ACS Appl. Mater. Interfaces* **2015**, *7*, 7251−63.

(16) Wu, W.; Yang, Y.; Zhou, H.; Ye, T.; Huang, Z.; Liu, R.; Kuang, Y. Highly Efficient Removal of Cu(II) from Aqueous Solution by Using Graphene Oxide. *Water, Air, Soil Pollut.* **2013**, *224*, 1372−1380.

(17) Yang, J.; Wu, J. X.; Lü, Q. F.; Lin, T. T. Facile Preparation of Lignosulfonate−Graphene Oxide−Polyaniline Ternary Nanocomposite as an Effective Adsorbent for Pb(II) Ions. *ACS Sustainable Chem. Eng.* **2014**, *2*, 1203−1211.

(18) Yang, Y.; Xie, Y.; Pang, L.; Li, M.; Song, X.; Wen, J.; Zhao, H. Preparation of reduced graphene oxide/poly(acrylamide) nanocomposite and its adsorption of Pb(II) and methylene blue. *Langmuir* **2013**, *29*, 10727−10736.

(19) Zhang, F.; Wang, B.; He, S.; Man, R. Preparation of Graphene-Oxide/ Polyamidoamine Dendrimers and Their Adsorption Properties toward Some Heavy Metal Ions. *J. Chem. Eng. Data* **2014**, *59*, 1719−1726.

(20) Gu, X. Y.; Yang, Y.; Hu, Y.; Hu, M.; Wang, C. Y. Fabrication of graphene-based xerogels for removal of heavy metal ions and capacitive deionization. *ACS Sustainable Chem. Eng.* **2015**, *3*, 1056−1065.

(21) Hu, X. J.; Liu, Y. G.; Wang, H.; Zeng, G. M.; Hu, X.; Guo, Y. M.; Li, T. T.; Chen, A. W.; Jiang, L. H.; Guo, F. Y. Adsorption of copper by magnetic graphene oxide-supported β-cyclodextrin: Effects of pH, ionic strength, background electrolytes, and citric acid. *Chem. Eng. Res. Des.* **2015**, *93*, 675−683.

(22) Mejias Carpio, I. E.; Mangadlao, J. D.; Nguyen, H. N.; Advincula, R. C.; Rodrigues, D. F. Graphene oxide functionalized with ethylenediamine triacetic acid for heavy metal adsorption and anti-microbial applications. *Carbon* **2014**, *77*, 289−301.

(23) Madadrang, C. J.; Kim, H. Y.; Gao, G.; Wang, N.; Zhu, J.; Feng, H.; Gorring, M.; Kasner, M. L.; Hou, S. Adsorption behavior of EDTA-graphene oxide for Pb (II) removal. *ACS Appl. Mater. Interfaces* **2012**, *4*, 1186−1193.

(24) Zhao, F.; Repo, E.; Sillanpää, M.; Meng, Y.; Yin, D.; Tang, W. Z. Green Synthesis of Magnetic EDTA- and/or DTPA-Cross-Linked

DOI: 10.1021/acs.jced.6b00746
J. Chem. Eng. Data 2017, 62, 407−416

Chitosan Adsorbents for Highly Efficient Removal of Metals. *Ind. Eng. Chem. Res.* **2015**, *54*, 1271−1281.
(25) Hong, P. K. A.; Li, C.; Banerji, S. K.; Wang, Y. Feasibility of metal recovery from soil using DTPA and its biostability. *J. Hazard. Mater.* **2002**, *94*, 253−272.
(26) Luo, S.; Xu, X.; Zhou, G.; Liu, C.; Tang, Y.; Liu, Y. Amino siloxane oligomer-linked graphene oxide as an efficient adsorbent for removal of Pb(II) from wastewater. *J. Hazard. Mater.* **2014**, *274*, 145−55.
(27) Hu, X. J.; Liu, Y. G.; Wang, H.; Chen, A. W.; Zeng, G. M.; Liu, S. M.; Guo, Y. M.; Hu, X.; Li, T. T.; Wang, Y. Q.; Zhou, L.; Liu, S. H. Removal of Cu(II) ions from aqueous solution using sulfonated magnetic graphene oxide composite. *Sep. Purif. Technol.* **2013**, *108*, 189−195.
(28) Hummers, W. S.; Offeman, R. E. Preparation of Graphitic Oxide. *J. Am. Chem. Soc.* **1958**, *80*, 1339.
(29) Guo, F. Y.; Liu, Y. G.; Wang, H.; Zeng, G. M.; Hu, X. J.; Zheng, B. H.; Li, T. T.; Tan, X. F.; Wang, S. F.; Zhang, M. M. Adsorption behavior of Cr(VI) from aqueous solution onto magnetic graphene oxide functionalized with 1,2-diaminocyclohexanetetraacetic acid. *RSC Adv.* **2015**, *5*, 45384−45392.
(30) Fan, L.; Luo, C.; Sun, M.; Li, X.; Lu, F.; Qiu, H. Preparation of novel magnetic chitosan/graphene oxide composite as effective adsorbents toward methylene blue. *Bioresour. Technol.* **2012**, *114*, 703−706.
(31) Zeng, W.; Liu, Y. G.; Hu, X. J.; Liu, S. B.; Zeng, G. M.; Zheng, B. H.; Jiang, L. H.; Guo, F. Y.; Ding, Y.; Xu, Y. Decontamination of methylene blue from aqueous solution by magnetic chitosan lignosulfonate grafted with graphene oxide: effects of environmental conditions and surfactant. *RSC Adv.* **2016**, *6*, 19298−19307.
(32) Li, L.; Fan, L.; Sun, M.; Qiu, H.; Li, X.; Duan, H.; Luo, C. Adsorbent for hydroquinone removal based on graphene oxide functionalized with magnetic cyclodextrin-chitosan. *Int. J. Biol. Macromol.* **2013**, *58*, 169−175.
(33) Depan, D.; Girase, B.; Shah, J. S.; Misra, R. D. Structure-process-property relationship of the polar graphene oxide-mediated cellular response and stimulated growth of osteoblasts on hybrid chitosan network structure nanocomposite scaffolds. *Acta Biomater.* **2011**, *7*, 3432−3445.
(34) Siva, T.; Kamaraj, K.; Karpakam, V.; Sathiyanarayanan, S. Soft template synthesis of poly(o-phenylenediamine) nanotubes and its application in self healing coatings. *Prog. Org. Coat.* **2013**, *76*, 581−588.
(35) Liu, J.; Chen, G.; Jiang, M. Supramolecular Hybrid Hydrogels from Noncovalently Functionalized Graphene with Block Copolymers. *Macromolecules* **2011**, *44*, 7682−7691.
(36) Duan, C.; Zhao, N.; Yu, X.; Zhang, X.; Xu, J. Chemically modified kapok fiber for fast adsorption of Pb^{2+}, Cd^{2+}, Cu^{2+} from aqueous solution. *Cellulose* **2013**, *20*, 849−860.
(37) Deng, J. H.; Zhang, X. R.; Zeng, G. M.; Gong, J. L.; Niu, Q. Y.; Liang, J. Simultaneous removal of Cd(II) and ionic dyes from aqueous solution using magnetic graphene oxide nanocomposite as an adsorbent. *Chem. Eng. J.* **2013**, *226*, 189−200.
(38) Hao, Y. M.; Man, C.; Hu, Z. B. Effective removal of Cu(II) ions from aqueous solution by amino-functionalized magnetic nano-particles. *J. Hazard. Mater.* **2010**, *184*, 392−399.
(39) Mi, X.; Huang, G.; Xie, W.; Wang, W.; Liu, Y.; Gao, J. Preparation of graphene oxide aerogel and its adsorption for Cu^{2+} ions. *Carbon* **2012**, *50*, 4856−4864.
(40) Zhang, F.; Wang, B.; He, S.; Man, R. Preparation of Graphene Oxide/ Polyamidoamine Dendrimers and Their Adsorption Properties toward Some Heavy Metal Ions. *J. Chem. Eng. Data* **2014**, *59*, 1719−1726.
(41) Jiang, Y.; Pang, H.; Liao, B. Removal of copper(II) ions from aqueous solution by modified bagasse. *J. Hazard. Mater.* **2009**, *164*, 1−9.
(42) Guo, X.; Du, B.; Wei, Q.; Yang, J.; Hu, L.; Yan, L.; Xu, W. Synthesis of amino functionalized magnetic graphenes composite material and its application to remove Cr(VI), Pb(II), Hg(II), Cd(II) and Ni(II) from contaminated water. *J. Hazard. Mater.* **2014**, *278*, 211−220.
(43) Gollavelli, G.; Chang, C. C.; Ling, Y. C. Facile synthesis of smart magnetic graphene for safe drinking water: heavy metal removal and disinfection control. *ACS Sustainable Chem. Eng.* **2013**, *1*, 462−472.
(44) Fan, L.; Luo, C.; Sun, M.; Li, X.; Qiu, H. Highly selective adsorption of lead ions by water-dispersible magnetic chitosan/graphene oxide composites. *Colloids Surf., B* **2013**, *103*, 523−9.
(45) Tan, M.; Liu, X.; Li, W.; Li, H. Enhancing Sorption Capacities for Copper(II) and Lead(II) under Weakly Acidic Conditions by L-Tryptophan-Functionalized Graphene Oxide. *J. Chem. Eng. Data* **2015**, *60*, 1469−1475.
(46) He, S. F.; Zhang, F.; Cheng, S. Z.; Wang, W. Synthesis of sodium acrylate and acrylamide copolymer/GO hydrogels and their effective adsorption for Pb^{2+} and Cd^{2+}. *ACS Sustainable Chem. Eng.* **2016**, *4*, 3948−3959.
(47) Moradi, O.; Zare, K.; Monajjemi, M.; Yari, M.; Aghaie, H. The Studies of Equilibrium and Thermodynamic Adsorption of Pb(II), Cd(II) and Cu(II) Ions From Aqueous Solution onto SWCNTs and SWCNT − COOH Surfaces. *Fullerenes, Nanotubes, Carbon Nanostruct.* **2010**, *18*, 285−302.
(48) Silva, V. L.; Carvalho, R.; Freitas, M. P.; Tormena, C. F.; Melo, W. C. Spectrometric and theoretical investigation of the structures of Cu and Pb/DTPA complexes. *Struct. Chem.* **2007**, *18*, 605−609.

DOI: 10.1021/acs.jced.6b00746
J. Chem. Eng. Data 2017, 62, 407−416